energies

MDPI

Article

Evolution of Mechanical Properties with Time of Fly-Ash-Based Geopolymer Mortars under the Effect of Granulated Ground Blast Furnace Slag Addition

Mateusz Sitarz [1,*], Izabela Hager [1] and Marta Choińska [2]

[1] Chair of Building Materials Engineering, Faculty of Civil Engineering, Cracow University of Technology, 24 Warszawska St. 31-155 Cracow, Poland; ihager@pk.edu.pl

[2] Nantes University—IUT Saint-Nazaire, Research Institute in Civil and Mechanical Engineering GeM–UMR CNRS 6183, 58, rue Michel Ange, 44 600 Saint Nazaire, France; marta.choinska@univ-nantes.fr

* Correspondence: mateusz.sitarz@pk.edu.pl; Tel.: +48-126-282-367

Received: 23 January 2020; Accepted: 2 March 2020; Published: 3 March 2020

Abstract: Geopolymers are considered to alternatives to Portland cement, providing an opportunity to exploit aluminosilicate wastes or co-products with promising performances in the construction sector. This research is aimed at investigating the strength of fly-ash-geopolymers of different ages. The effect of granulated blast furnace slag (GGBFS) as a partial replacement of fly ash (FA) on the tensile (f_t) and compressive strength (f_c), as well as the modulus of elasticity, is investigated. The main advantage of the developed geopolymer mixes containing GGBFS is their ability to set and harden at room temperature with no need for heating to obtain binding properties, reducing the energy consumption of their production processes. This procedure presents a huge advantage over binders requiring heat curing, constituting a significant energy savings and reduction of CO_2 emissions. It is found that the development of strength strongly depends on the ratio of fly-ash to granulated blast furnace slag. With the highest amount of GGBFS, the compressive strength of geopolymers made of fly-ash reached 63 MPa after 28 days of curing at ambient temperature. The evolution of compressive strength with time is correlated with the development of ultrasound pulse velocity methods, which are used to evaluate maturity. The modulus of elasticity changes with strength and the relationship obtained for the geopolymer is presented on the basis of typical models used for cement-based materials. The tensile to compressive strength ratios of the tested geopolymers are identified as higher than for cementitious binders, and the $f_t(f_c)$ relationship is juxtaposed with dependencies known for cement binders, showing that the square root function gives the best fit to the results.

Keywords: fly-ash-based geopolymer; FA; GGBFS; UPV; mechanical properties; geopolymer elasticity

1. Introduction

Geopolymers and alkali-activated aluminosilicates are considered sustainable alternatives to Portland cement, providing an opportunity to exploit wastes or co-products with promising performances in the construction sector [1–4]. Their production requires metakaolinite or industrial waste materials containing aluminosilicates, such as fly-ash (FA) and granulated ground blast furnace (GGBFS) [2]. Aluminosilicates for geopolymer manufacturing can be readily found, either as raw minerals or in widely available waste streams. Under highly alkaline conditions, these raw materials have binding properties which allow for the synthesis of strong and durable composites [3,4]. Numerous studies have been carried out to provide more insight into the method of synthesis and the best composition thereof [5,6]. Nevertheless, there is still a great need to provide more data for the

development of methods for designing geopolymers. The geopolymerization process is strongly dependent on the source, composition, and particle size of the aluminosilicates; thus, a database on the chemistry, reactivity, and dissolution mechanisms of various precursors must be completed [5]. There are many examples of geopolymer mixes and alkali-activated materials (AAM) in the literature. The properties of those binders depend on the chemical composition of the source material (precursor) [7]. High- and low-calcium alumicosilicates have been considered. Aluminosilicate systems based on FA with low calcium content require a heat treatment curing cycle, which makes these materials well suited for prefabrication and precast manufacturing processes [8–11], but they jeopardize their sustainable character because they require a significant amount of thermal energy to set and harden. Previous studies by the authors have reported that the setting of fly-ash-based geopolymers was considerably delayed when cured at room temperature. Demoulding was only possible after 3 days and the mechanical performance of the fly-ash-based geopolymer was low [11].

It has been reported that the structure of geopolymer binders synthesized at ambient temperature is amorphous [12]; with increasing temperature, crystalline phases begin to appear [13]. The mechanism of setting and hardening geopolymer binder is a complex process. The most important factors determining the type and the amount of amorphous (gel-like) or crystalline structures formed are the raw materials and the conditions in which the reaction take place [14]. Furthermore, the structure of the hardened geopolymer is made up of polymerization reaction products and unreacted elements of the precursor. For blended binders, the problem is even more complex. Products resulting from the dissolution of FA and GGBFS in an alkaline medium may join with each other and chemically interact [15]. For this reason, quantitative and qualitative evaluation of the resulting geopolymer structure is required.On the basis of the works of [16], it may also be expected that geopolymers produced by the chemical activation of a blend of fly-ash and GGBFS may have the shared features of amorphous hydrated alkali-aluminosilicate(N-A-S-H) and calcium silicate hydrate(C-S-H) gel. According to the authors of [13,16], in the methods of synthesis for alkali-activated slags and geopolymers based on class F fly-ash (classification according to ASTM C618 [17] the geopolymerization products are different. The reaction product observed in case of the fly-ash-based geopolymer is amorphous hydrated alkali-aluminosilicate(N-A-S-H) [7,13,18] while, for alkali-activated slags, it is mainly calcium silicate hydrate gel. For amorphous hydrated alkali-aluminosilicates, calcium is not necessary for forming the geopolymer structure [16]. Moreover, according to [19], flexural strength is positively affected by the FA alkali reaction products, while the GGBFS alkali reaction products have a positive effect on compressive strength.

As the objective of this research is to manufacture sustainable materials based on fly-ash from the power plant with a dynamic increase in strength without the need to apply heat-curing, FA with high silica content (52.3 wt.%) and ground granulated blast furnace slag (GGBFS) are investigated. The GGBFSused in this research is characterized with a high calcium oxide content (43.9 wt.%).

In view of lowering the energy demand of the geopolymer production process, blends of fly-ash from power plant with granulated blast furnace slag were used in this research. This procedure allowed setting to be obtained at room temperature with no need for curing at an elevated temperature, which presents a huge advantage over binders requiring heat curing in order to bind them, constituting a significant energy saving and resulting in a reduction of CO_2 emissions.In this research, FA was blended with GGBFS at three levels of addition: 10, 30, and 50 wt.% was used as a partial replacement of the fly-ash content. The increase of GGBFS content in the fly-ash-based geopolymer affects setting time, the kinetics of strength development, and flexural and compressive strengths.

2. Materials and Methods

2.1. Materials

We used siliceous fly-ash provided by the power plant in Połaniec, southern Poland, and ground granulated blast furnace slag (GGBFS) provided by Ekocem, Poland. The main components of the

fly-ash were SiO_2 (52 wt.%) and Al_2O_3 (28 wt.%). In addition, the FA contained Fe_2O_3 and small amounts of MgO, K_2O, TiO_2, and Na_2O. The total content of silicon dioxide, alumina, and iron (III) oxide exceeded 70%. Due to this specific chemical composition, fly-ash was classified as a siliceous ash; based on the chemical analysis and according to EN 450-1:2012 [20], this FA can be classified as type II. According to ASTM C618 [17], the FA belongs to class F. The specific gravities of the fly-ash and ground granulated blast furnace slag (GGBFS) used were 2.1 g/cm^3 and 2.9 g/cm^3, respectively. Siliceous sand (0/2 mm) was used to prepare the geopolymer mortars. The chemical compositions of FA and GGBFS can be found in Tables 1 and 2, respectively.

Table 1. Analysis of fly-ash (FA). Oxides contents in wt.%.

SiO_2	Al_2O_3	Fe_2O_3	CaO	MgO	SO_3	K_2O	Na_2O	P_2O_5	TiO_2	Mn_3O_4
52.30	28.05	6.32	3.05	1.71	0.28	2.51	0.76	0.69	1.35	0.07

Table 2. Ground granulated blast-furnace slag (GGBFS)characteristics. Oxides contents in wt.%.

SiO_2	Al_2O_3	Fe_2O_3	CaO	MgO	SO_3	K_2O	Na_2O	Cl^-	Na_2Oeq	Blaine
39.31	7.61	1.49	43.90	4.15	0.51	0.356	0.468	0.038	0.702	3904

The most commonly available sodium silicate solutions are characterized by a molar module of about 2.6. For the production of geopolymers, it is necessary to use solutions with a lower module (i.e., 1.5–2.0) [21]. Hence, it is necessary to lower the module with a sodium hydroxide solution. In order to reduce the arduous process of regulating the molar ratio of sodium silicate solution with sodium hydroxide, specially developed aqueous silicate solutions dedicated to geopolymer materials were used. A soluble sodium silicate solution (called Na-Sil) supplied by Woellner was used. The product Geosil® 34417 has a molar ratio of 1.7. The Molar Ratio (MR) of a silicate solution is defined as the mole ratio of silica to sodium oxide in the solution. The chemical specification, according to the technical report supplied by the manufacturer, is shown in Table 3.

Table 3. Woellner Geosil silicate solution, data supplied by the producer.

Characteristic	Unit	Geosil 34417 (Na-Sil)
Na_2O	wt.%	16.74
SiO_2	wt.%	27.5
density	g/cm^3	1.552
viscosity	mPa.s	470
weight ratio (WR = wt.% SiO_2/wt.% Na_2O)	–	1.64
molar ratio (MR = mol SiO_2/molNa_2O)	–	1.70

The alkaline solution used in this research was a mixture of sodium silicate solution and additional water, which was necessary to obtain appropriate workability of the geopolymer mortars. The total amount of water determined for manufacturing the geopolymer mortars took into account the water contained in the liquid alkaline solution, and its composition is presented in Table 4.

Table 4. Composition of liquid alkaline solutionGeosil 34417 and water.

Component	Na_2O	SiO_2	H_2O
Percentage content [wt.%]	12.6	20.6	66.8

Table 5 shows the densitiesof all individual mortar components. Table 6 shows the weight of the amounts of individual ingredients needed to prepare 1 m^3 of each mortar. Individual mortar components are characterized by different densities. To obtain the same volume of mortar with a

change in the ratio between the mass of FA and GGBFS, the mass shares of other components must be adjusted. In order to provide a variable FA to GGBFS mass ratio, small changes in the amount of other ingredients per 1 m^3 of mortar were necessary, due to differences in density between FA and GGBFS.

Table 5. Densities of mortar components.

Mortar Component	Density (g/cm^3)
Fly-ash (FA)	2.10
GGBFS	2.90
Sand	2.65
Alkaline solution	1.41

Table 6. Mix compositions of geopolymer mortars 10N, 30N and 50N for 1 m^3 of mortar.

Components	10N	30N	50N
	(kg/m^3)	(kg/m^3)	(kg/m^3)
Alkaline solution (Na-Sil + extra water)	334.0	340.6	347.5
FA	667.9	529.8	386.1
GGBFS	74.2	227.1	386.1
Sand (0/2 mm)	1113.2	1135.3	1158.3
Mortar parameters			
sand to binder weight ratio (sand/FA + GGBFS)	1.5	1.5	1.5
alkaline solution to binder (FA + GGBFS) weight ratio	0.45	0.45	0.45
water to binder (FA + GGBFS) weight ratio	0.3	0.3	0.3

Three geopolymer mortars, named 10N, 30N, and 50N, were prepared. The numerical value in the label corresponds to the amount of GGBFS (in percentage). The binder was considered as the sum of the fly-ash and ground granulated blast furnace slag contents (FA + GGBFS) in weight. Three main indices were set as constant when designing the geopolymer mortar's composition: sand to binder weight ratio, alkaline solution to binder weight ratio, and water to binder weight ratio (shown in Table 6). The mix compositions and constant parameters characterizing all prepared mortars are given, in detail, in Table 6.

Adequate workability was achieved with all the materials, enabling the mixing and casting of all the samples. Prismatic samples of dimensions 40 × 40 × 160 mm were cast in plastic molds and compacted at a shaking table. The thixotropic behavior of the mortars was observed during compaction. The molds were covered with a plastic lid and cured at room temperature (18 °C). After 1 day, the samples were removed from the molds and stored in plastic bags for 7 days, in order to prevent moisture loss during curing. Afterwards, the samples were stored in laboratory conditions (T = 18 ± 2 °C, RH = 75%) until the mechanical tests were performed.

2.2. Methodology

All physical (density, porosity, and ultrasonic pulse velocities) and mechanical (compressive and flexural tensile strength) properties of the hardened mortars were tested over time spans to monitor their evolution during curing. Each specimen was subjected to a constant load rate (50 N/s) in three-point bending to determine flexural tensile strength. The remaining mortar prisms from the bending test were used for the determination of compressive strength on a hydraulic press, according to the standard procedure for cement mortar with a constant load rate (2400 N/s). The tests were carried out at 1, 3, 7, 14, and 28 days on 3 samples.

In this research, the velocities of ultrasonic pulses in geopolymers of different ages were investigated in all samples subjected to the compression test. The measurements were performed using a Portable

Ultrasonic Non-Destructive Digital Indicating Tester (PUNDIT) plus (Proceq, Switzerland). Cylindrical transducers with a nominal frequency of 54 kHz were applied in the geopolymer investigation. The values of ultrasonic pulse velocities in mortars UPV were evaluated on the basis of time of flight: the offset point on an amplitude–time curve (Figure 1). The elastic wave velocity, V, in the material is a good indicator of its quality, due to the sensitivity of wave velocities to air voids, cracks, and the presence of pores. UPV measurement is the one of various non-destructive testing methods which have been used to evaluate material quality and maturity [22]. The evolution of UPV with time is a good indicator for observing setting time [23] maturity or the degree of damage to a mineral material [24].

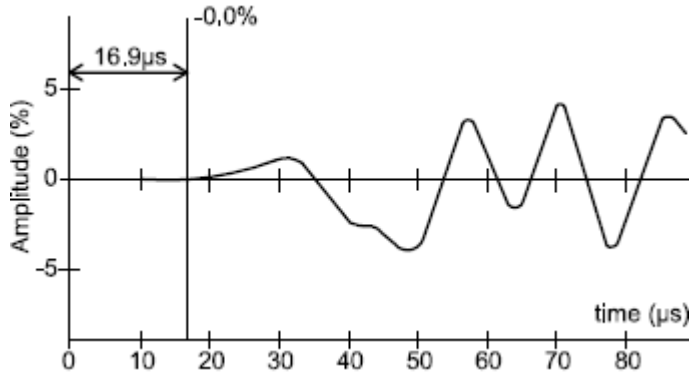

Figure 1. Ultrasonic pulse velocity time of flight: the off-set point on the amplitude–time curve.

In addition, the dynamic modulus of elasticity, E_d, was determined using the Formula (1), presenting the relationship between the velocity of the primary elastic wave (V), dynamic modulus of elasticity (E_d), apparent density (ρ_o), and Poisson ratio (ν) of the tested material:

$$V = \sqrt{\frac{Ed(1-\nu)}{\rho_o(1+\nu)(1-2\nu)}} \quad (1)$$

From the amplitude–time curve (Figure 1), the time of flight of the ultrasonic pulse is determined with an accuracy of 0.1 µs and the primary wave velocity (V) is calculated usingthe known distance between transducers. The apparent density changes over time were measured for all the samples tested. The Poisson ratio was assumed to be 0.2.

The tests were performed with the objective of determining how V changes with time, identifying the relationship between f_c(V) and f_t (V), and determining the static and dynamic moduli of elasticity (E, E_d), as well as verifying the modulus variation along with the strength variation, $E_d(f_c)$.The $E(f_c)$ results were noted and compared with relationships available in the literature and codes.

3. Results and Discussion

3.1. Density and Porosity

The mean values of apparent density (ρ) and UPV (V), as well as relative changes of density, are presented in Table 7. It can be seen that higher GGBFS content induced an increase in density, due to less porous structure development. The change of mass due to drying is progressive, so the apparent density changes as a function of time.

Table 7. Apparent densities of geopolymer mortars 10N, 30N, and 50N at different ages.

Mean Values of Apparent Density	10N (kg/m^3)	30N (kg/m^3)	50N (kg/m^3)
1d	2051	2141	2223
3d	2047	2137	2215
7d	2043	2133	2211
14d	2027	2121	2210
28d	2012	2113	2207

Furthermore, after 28 days, pore size distribution was measured with mercury intrusion porosimetry (MIP), detecting open pores between 3.5 nm and 500 µm. The mercury intrusion porosimetry provides the option to measureintruded mercury volume, providing information about the pore volume and size [25,26]. For each material, three specimens were prepared, and the mean values are presented in Figure 2a,b. Total porosity was deducted from the cumulative intrusion of mercury pictograms Figure 2a.

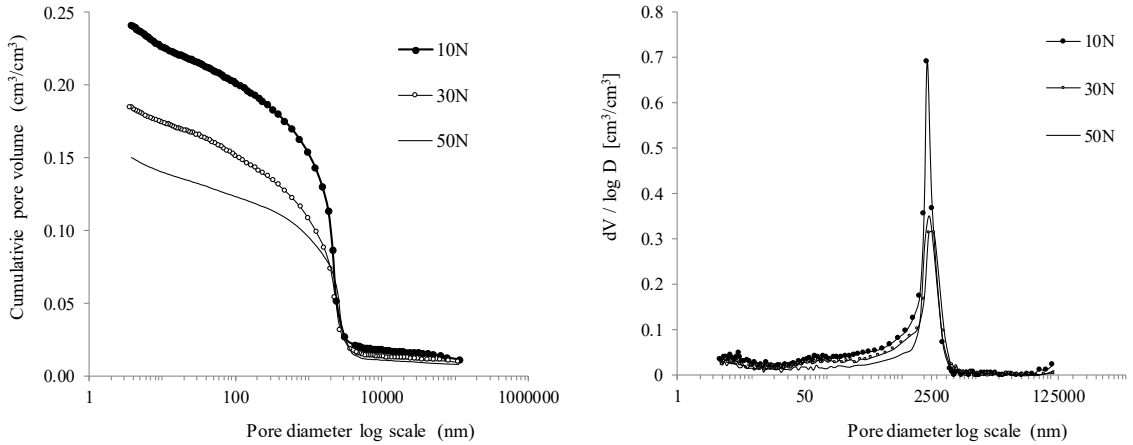

(a) **(b)**

Figure 2. (**a**): Total porosity of geopolymer mortars 10N, 30N and 50N (**b**): Pore size distribution of geopolymer mortars.

For 10N, 30N, and 50N geopolymer mortar samples, the total porosity reached values of 0.240, 0.184, and 0.145 cm^3/cm^3, respectively. The addition of higher content of GGBFS resulted in lower porosity and a denser structure.In the results of other studies, geopolymers have been characterized by pore size distribution resembling a bell curve centred in the mesoporous region [27,28]. The geopolymer mortars 10N, 30N, and 50N all presented a bell curve shape with one clear peak, situated at 2230 nm, 2054 nm, and 3127 nm, respectively (Figure 2b). The peak was particularly pronounced for samples with a 10% addition of GGBFS. The results show that, in the case of the tested geopolymer mortars, macropores were dominant.

3.2. Compressive Strength and Flexural Tensile Strength

We investigated the relationship between the flexural tensile strength and compressive strength of geopolymer fly-ash-based mortars. It can be observed, from Figure 3a,b, that the flexural tensile strength and compressive strengths of the tested geopolymer mortars were significantly dependent on the FA–GGBFS blending proportion.An increase of the GGBFS content induced an increase of compressive strength. The 50N composition (50% FA and 50% GGBFS) demonstrated the highest mechanical performance, where compressive strength reached 63.5 MPa and flexural tensile strength was 6.5 MPa.

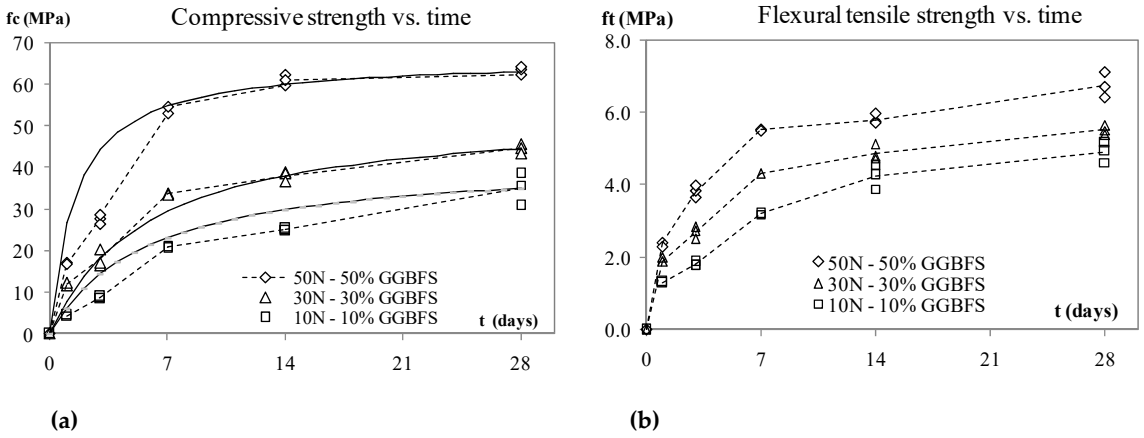

Figure 3. (**a**): Evolution of compressive strength as a function of curing time and comparison with EUROCODE (**b**): Evolution of flexural tensile strength as a function of curing time.

The evolution of compressive strength for 50N and 10N was slower than for cementitious material, as shown in Figure 4 and described by the following equations originating from EUROCODE EN 1992-1, where d means day:

$$f_{cd} = d \cdot f_{c28d} / (4.76 + 0.83\ d)\ d\ \leq 28 \text{ and } fc_{28}\ \leq\ 40 \text{ MPa} \quad (2)$$

$$f_{cd} = d \cdot f_{c28d} / (1.40 + 0.95\ d) d\ \leq 28 \text{ and } fc_{28} >\ 40 \text{ MPa} \quad (3)$$

The flexural strength of tested geopolymer mortars investigated also strongly depended on the blend composition. An increase of GGBFS content positively affected the flexural tensile strength results of the mortars. An increase of up to 30% GGBFS induced an increase in tensile strength. The highest strength at day 3 was for 50N; for this mortar, the flexural tensile strength at 14 and 28 days reached 2.8 MPa and 6.8 MPa, respectively.

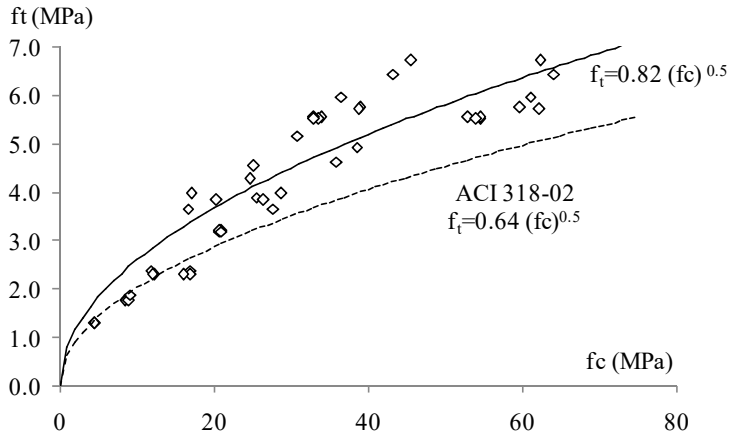

Figure 4. The $f_t(f_c)$ relationships for fly-ash geopolymer mortars 10N, 30N, and 50N, compared with the ACI 318-02 square root equation for geopolymer binders.

In Figure 4, all compressive and tensile strength results are presented, along with the $f_t(f_c)$ relationship proposed in ACI 318-02 [29] for ordinary Portland cement concretes (4):

$$ft = 0.64\ \sqrt{fc} \quad (4)$$

In this research, a formula similar to ACI 318-02, a square root function with coefficient 0.82 (proposed as Equation (5)) covered the results obtained for the 10N, 30N, and 50N geopolymer

mortars.These results agree with what was reported by the authors of [30], that these materials present higher tensile to compressive strength ratios than when using Portland cement binder.

$$ft = 0.82\ \sqrt{fc} \quad (5)$$

3.3. Evolution of Ultrasonic Pulse Velocity and Modulus of Elasticity of Tested Materials

The variation in ultrasonic pulse velocity (UPV) and the dynamic modulus of elasticity over time was determined on the basis of elastic wave (m/s) values measured using PUNDIT on the geopolymer mortars. All results are presented in Figure 6. The UPV measurements were started at 24 h after casting, when the samples were removed from the molds. The ultrasonic pulse velocity values for 10N, 30N, and 50N at 24 h reached 2226 m/s, 2899 m/s, and 3167 m/s, respectively. After 14 days, the values reached 3270 m/s, 3909 m/s, and 4300 m/s correspondingly for 10N, 30N, and 50N. The increase in ultrasonic pulse velocities followed the maturity and strength development curves.

The dynamic modulus of elasticity E_d was determined using Formula (1) and the static modulus of elasticity E was calculated using the empirical relation (6) proposed by [31]. For this purpose, the dynamic modulus was converted to the elastic one using a multiplying factor of 0.83 (-).

$$E = 0.83\ E_d \quad (6)$$

It was observed that, in a similar manner to the evolution of compressive strength, the V values at 14 and 28 days were similar, showing the stabilization of mechanical performance after 14 days (see Figure 3a,b and also Figure 5a,b).

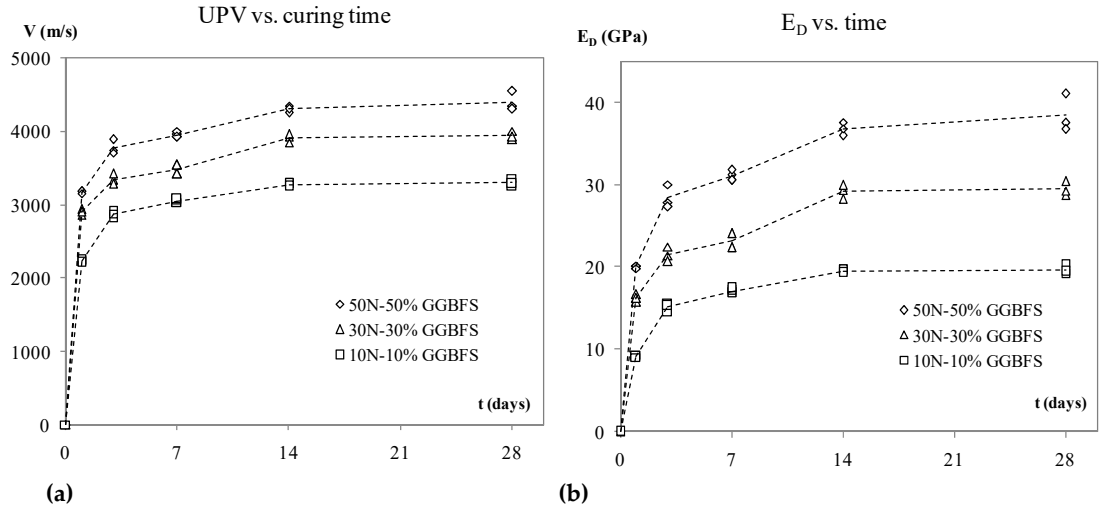

Figure 5. (**a**): Evolution of UPV as a function of curing time (**b**): Dynamic modulus of elasticity E_d as a function of curing time.

After these initial observations, actions were taken to determine the changes in the dynamic and static moduli of elasticity and to compare them with the dependencies which can be found in the literature for cementitious materials. The evolution of the dynamic modulus of elasticity over time presented similar tendencies over time to V(t).

To establish the correlation of compressive and flexural tensile strength with the ultrasonic pulse velocity V: $f_t(V)$ and $f_c(V)$ relationships for the test geopolymers, all data of the three sets of samples prepared from 10N, 30N, and 50N are plotted in Figure 6a,b. The experimental results presented here show that the compressive and flexural tensile strengths were strongly correlated with the ultrasonic pulse velocity of geopolymer mortars. Moreover, these relationships were significantly influenced

by the age of the tested mortars. Polynomial functions were proposed, similar to those presented for cementitious binders (European Standard EN-12504 [32]) with a correlation factor (R^2) higher than 0.7.

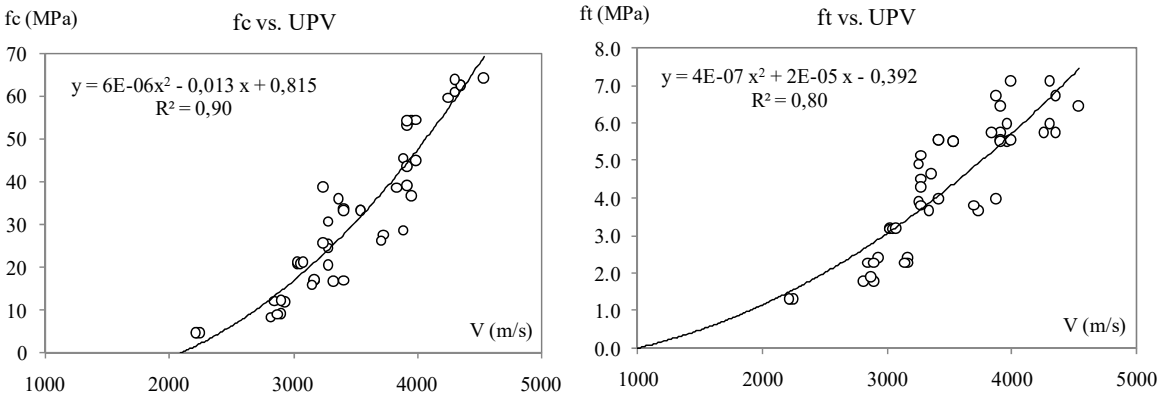

(a) **(b)**

Figure 6. (**a**): The correlation of compressive strength with the ultrasonic pulse velocity f_c(V (**b**): The correlation of flexural tensile strength with the ultrasonic pulse velocity f_t(V). The f_c(V) and f_t(V) relationships for fly-ash geopolymer mortars 10N, 30N, and 50N; all results obtained collectively after 1, 3, 7, 14, and 28 days.

Furthermore, in order to provide some issues for the future standardization of geopolymers for construction purposes, we investigated the relationship between the variation of modulus of elasticity and compressive strength.

The results were also compared with the International Federation for Structural Concrete (FIB) [33] and EC2 (Eurocode 2) [34] models for cement concrete. The FIB model considers that the modulus of elasticity at 28 days E_{ct} is determined by (7), where $E_{c0} = 21.5 \cdot 10^3$ MPa, α_E =1.0 for quartzite aggregates, and f_{cm} is the characteristic strength (in MPa):

$$E_{ct} = E_{c0} \cdot \alpha_E \cdot \left(\frac{f_{cm}}{10}\right)^{\frac{1}{3}} \quad (7)$$

The EC2 model considers the modulus of elasticity at 28 days $E_{cm}$to be determined by (8), where f_{cm} is the characteristic strength (in MPa):

$$E_{cm} = 22\,[(f_{cm})/10]^{0.33} \quad (8)$$

As can be seen from Figure 7, the obtained experimental results were shifted down in comparison with the FIB model code, as well as in comparison to the Eurocode 2 model. Both models (FIB and EC2) overestimate the elastic modulus and need to be reviewed for geopolymer-type binders, represented here by the fly-ash-based geopolymers.

One may observe that this evolution follows a power law, similar to the one proposed already for concrete by the AIJ (Architecture Institute of Japan) and used by Tomosawa and Noguchi [35], see Equation (9):

$$E = 2.1 \cdot 10^5 \left(\frac{\gamma}{2.3}\right)^{1.5} \left(\frac{f_c}{200}\right)^{\frac{1}{2}} \quad (9)$$

Where E stands for the modulus of elasticity (kgf/cm^2), γ is density of concrete (t/m^3), and f_c refers to the compressive strength value of concrete (kgf/cm^2). The modulus thus obtained was converted to GPa (see Figure 7).

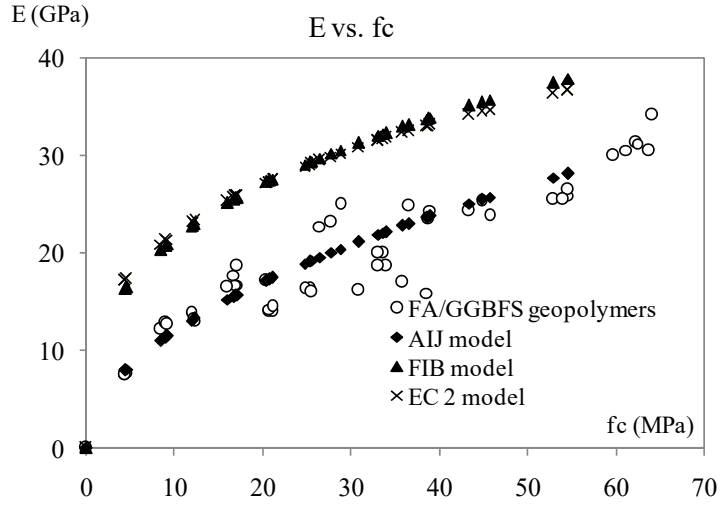

Figure 7. Static elastic modulus of elasticity evolution with compressive strength for the fly ash and ground granulated blast furnace slag blended geopolymer mortars 10N, 30N, and 50N, in comparison with $E(f_c)$ models for cementitious materials.

4. Conclusions

This study demonstrated how the addition of GGBFS to FA-based geopolymers affects the evolution of the strength of the resultant geopolymer mortars. Blending GGBFS with FA makes it possible to manufacture sustainable material which is able to set at ambient temperature, with no additional temperature curing.

The strength-increase kinetics of fly-ash-based geopolymers using FA from thePołaniec power plant were strongly dependent on the GGBFS content. Based on the results, the following observations were made:

- For the mortars cured at room temperature, the addition of a higher GGBFS content resulted in an increase in both compressive and tensile strength;
- Blending of FA (silica content 52.3 wt.%) with GGBFS (calcium oxide 43.9 wt.%) enabled us to obtain strength development kinetics similar to those observed for cement-based materials (Figure 4);
- The mechanical properties of compressive and flexural tensile strength of the mortars increased along with an increase in the amount of GGBFS. The best performances at 28 days were obtained by the 50N mortar (50% FA and 50% GGBFS), reaching fc = 63 MPa and ft = 6.8 MPa;
- Relatively high values of flexural tensile strength were observed for all the FA-based geopolymer mortars tested.Moreover, tensile to compressive strength ratios were higher than those of Portland cement composites and the $f_t(f_c)$ relationships proposed for fly-ash geopolymer mortars were of a similar form to that given in the ACI 318-02;
- Ultrasonic pulse velocity measurements are an effective method for evaluating the maturity of a geopolymer and correlate well with the evolution of their mechanical properties over time;
- In a similar manner to the evolution of compressive strength, the UPV values tend to stabilize after 7 days;
- For FA-based geopolymers with the addition of GGBFS, the polynomial relationships $f_c(V)$ and $f_t(V)$ were proposed. These relations can be used to evaluate the maturity or damage to geopolymer mortars;
- For all materials tested, the values of the dynamic modulus of elasticity were calculated on the basis of UPV measurements andthe static modulus of elasticity values E were evaluated.A unique power law was provided for all the materials tested, in order to determine the variation in elastic modulus as a function of compressive strength $E(f_c)$; and

- The results show that the EC2 and FIB formulae may not be suitable to evaluate the E(f_c) relations and tend to overestimate the modulus of elasticity inFA-based geopolymer binders of a given strength.

The scope of applicability of the dependencies determined in this study is adequate for FA–GGBFS blended precursors and geopolymer mortars cured at ambient temperature. Further research is needed to determine similar relationships in geopolymer binders based on other types of precursors and activators.

Author Contributions: Conceptualization, I.H.; Methodology, M.S. and I.H.; Formal Analysis, M.C.; Founding Acquisition, I.H.; Investigation Data Curation, M.S., I.H. and M.C.; Writing—Original Draft Preparation, M.S., I.H. and M.C.; Supervision, I.H.; Validation, M.S., M.C. and I.H.; Writing—Review and Editing, M.S. and I.H. All authors have read and agreed to the published version of the manuscript.

Funding: This research was supported and funded in part from the EMMAT project E-mobility and sustainable materials and technologies PPI/APM/2018/1/00027 financed by the Polish National Agency for Academic Exchange (NAWA).

Conflicts of Interest: The authors declare no conflict of interest.

References

1. Ma, C.-K.; Awang, A.Z.; Omar, W. Structural and material performance of geopolymer concrete: A review. *Constr. Build. Mater.* **2018**, *186*, 90–102. [CrossRef]
2. Bai, T.; Song, Z.; Wang, H.; Wu, Y.; Huang, W. Performance evaluation of metakaolin geopolymer modified by different solid wastes. *J. Clean. Prod.* **2019**, *226*, 114–121. [CrossRef]
3. Saha, S.; Rajasekaran, C. Enhancement of the properties of fly ash based geopolymer paste by incorporating ground granulated blast furnace slag. *Constr. Build. Mater.* **2017**, *146*, 615–620. [CrossRef]
4. Albitar, M.; Mohamed Ali, M.S.; Visintin, P.; Drechsler, M. Durability evaluation of geopolymer and conventional concretes. *Constr. Build. Mater.* **2017**, *136*, 374–385. [CrossRef]
5. Duxson, P.; Provis, J.L. Designing precursors for geopolymer cements. *J. Am. Ceram. Soc.* **2008**, *91*, 3864–3869. [CrossRef]
6. Naghizadeh, A.; Ekolu, S.O. Method for comprehensive mix design of fly ash geopolymer mortars. *Constr. Build. Mater.* **2019**, *202*, 704–717. [CrossRef]
7. Duxson, P.; Fernández-Jiménez, A.; Provis, J.L.; Lukey, G.C.; Palomo, A.; Van Deventer, J.S.J. Geopolymer technology: The current state of the art. *J. Mater. Sci.* **2007**, *42*, 2917–2933. [CrossRef]
8. Sitarz, M.; Hager, I.; Kochanek, J. Effect of High Temperature on Mechanical Properties of Geopolymer Mortar. In Proceedings of the MATBUD'2018—8th Scientific-Technical Conference on Material Problems in Civil Engineering, Cracow, Poland, 25–27 June 2018.
9. Fan, F.; Liu, Z.; Xu, G.; Peng, H.; Cai, C.S. Mechanical and thermal properties of fly-ash based geopolymers. *Constr. Build. Mater.* **2018**, *160*, 66–81. [CrossRef]
10. Bakharev, T. Thermal behaviour of geopolymers prepared using class F fly-ash and elevated temperature curing. *Cem. Concr. Res.* **2006**, *36*, 1134–1147. [CrossRef]
11. Sitarz, M.; Hager, I. Twelfth International Symposium On Brittle Matrix Composites. In Proceedings of the Effect Of Addition Of Limestone Powder On Fly-Ash Based Geopolymer Cured At 80 °C And At Ambient Temperature, Warsaw, Poland, 23–24 September 2019.
12. Palomo, A.; Alonso, S.; Femandez-Jimenez, A. Alkaline activation of fly-ashes: NMR study of the reaction products. *J. Am. Cem. Soc.* **2004**, *87*, 1141–1145. [CrossRef]
13. Khale, D.; Chaudhary, R. Mechanism of Geopolymerization and Factors Influencing Its Development: A Review. *J. Mater. Sci.* **2007**, *42*, 729–746. [CrossRef]
14. Mustafa Al Bakri, A.M.; Kamarudin, H.; Bnhussain, M.; Nizar, I.K.; Mastura, W.I.W. Mechanism and Chemical Reaction of Fly-Ash Geopolymer Cement-A Review. *J. Chem. Inf. Model.* **2013**, *53*, 1689–1699.
15. Lloyd, R.R.; Provis, J.L.; Van Deventer, J.S.J. Microscopy and microanalysis of inorganic polymer cements. 2: The gel binder. *J. Mater. Sci.* **2009**, *44*, 620–631. [CrossRef]

16. Oh, J.E.; Monteiro, P.J.M.; Jun, S.S.; Choi, S.; Clark, S.M. The evolution of strength and crystalline phases for alkali-activated ground blast furnace slag and fly-ash-based geopolymers. *Cem. Concr. Res.* **2010**, *40*, 189–196. [CrossRef]
17. ASTM International. *ASTM C618-19—Standard Specification for Coal Fly Ash and Raw or Calcined Natural Pozzolan for Use in Concrete*; ASTM International: West Conshohocken, PA, USA, 2019.
18. Palomo, A.; Grutzeck, M.W.; Blanco, M.T. Alkali-activated fly ashes: A cement for the future. *Cem. Concr. Res.* **1999**, *29*, 1323–1329. [CrossRef]
19. Marjanović, N.; Komljenović, M.; Baščarević, Z.; Nikolić, V.; Petrović, R. Physical–mechanical and microstructural properties of alkali-activated fly-ash–blast furnace slag blends. *Ceram. Int.* **2015**, *41*, 1421–1435. [CrossRef]
20. Standards, EN 450-1-Fly-ash for concrete—Part 1: Definition, Specifications and Conformity Criteria. Available online: https://global.ihs.com/doc_detail.cfm?document_name=BS%20EN%20450%2D1&item_s_key=00463023&rid=IHS (accessed on 3 March 2020).
21. Davidovits, J. *Geopolymer Chemistry and Applications*, 4th ed.; Geopolymer Institute: Saint-Quentin, France, 2008; Volume 171, ISBN 9782951482098.
22. Ghosh, R.; Sagar, S.P.; Kumar, A.; Gupta, S.K.; Kumar, S. Estimation of geopolymer concrete strength from ultrasonic pulse velocity (UPV) using high power pulser. *J. Build. Eng.* **2018**, *16*, 39–44. [CrossRef]
23. Mohammed, T.U.; Rahman, M.N. Effect of types of aggregate and sand-to-aggregate volume ratio on UPV in concrete. *Constr. Build. Mater.* **2016**, *125*, 832–841. [CrossRef]
24. Picandet, V.; Khelidj, A.; Bastian, G. Effect of axial compressive damage on gas permeability of ordinary and high-performance concrete. *Cem. Concr. Res.* **2001**, *31*, 1525–1532. [CrossRef]
25. Giesche, H. Mercury Porosimetry. In *Handbook of Porous Solids*; John Wiley & Sons, Ltd.: Hoboken, NJ, USA, 2008; pp. 309–351.
26. Washburn, E.W. The Dynamics of Capillary Flow. *Phys. Rev.* **1921**, *17*, 273–283. [CrossRef]
27. Steins, P.; Poulesquen, A.; Frizon, F.; Diat, O.; Jestin, J.; Causse, J.; Lambertin, D.; Rossignol, S. Effect of aging and alkali activator on the porous structure of a geopolymer. *J. Appl. Crystallogr.* **2014**, *47*, 316–324. [CrossRef]
28. Medpelli, D.; Seo, J.-M.; Seo, D.-K. Geopolymer with Hierarchically Meso-/Macroporous Structures from Reactive Emulsion Templating. *J. Am. Ceram. Soc.* **2014**, *97*, 70–73. [CrossRef]
29. Tuan, T.M. ACI 318-02. *Practice. Concr. Int.* **2003**, *25*, 71–75.
30. Farhan, N.A.; Sheikh, M.N.; Hadi, M.N.S. Investigation of engineering properties of normal and high strength fly-ash based geopolymer and alkali-activated slag concrete compared to ordinary Portland cement concrete. *Constr. Build. Mater.* **2019**, *196*, 26–42. [CrossRef]
31. Lydon, F.D.; Balendran, R.V. Some observations on elastic properties of plain concrete. *Cem. Concr. Res.* **1986**, *16*, 314–324. [CrossRef]
32. European Standards EN 12504-1—Testing Concrete in Structures—Part 1: Cored Specimens—Taking, Examining and Testing in Compression. Available online: https://global.ihs.com/doc_detail.cfm?document_name=BS%20EN%2012504%2D1&item_s_key=00348183 (accessed on 3 March 2020).
33. International Federation for Structural Concrete Model Code 2010 (Final Version). fib Bull. 2012, 65 & 66. Available online: https://www.ernst-und-sohn.de/index.php?q=en/fib-model-code-for-concrete-structures-2010 (accessed on 3 March 2020).
34. European standards EN 1992-1—Design of Concrete Structures General Rules and Rules for Buildings. Available online: https://www.phd.eng.br/wp-content/uploads/2015/12/en.1992.1.1.2004.pdf (accessed on 3 March 2020).
35. Tomosawa, F.; Noguchi, T. Relationship Between Compressive Strength And Modulus Of Elasticity Of High-Strength Concrete. *J. Struct. Constr. Eng.* **1995**, *60*, 1–10.